Loughborough
University

This item was submitted to Loughborough's Institutional Repository (https://dspace.lboro.ac.uk/) by the author and is made available under the following Creative Commons Licence conditions.

For the full text of this licence, please go to:
http://creativecommons.org/licenses/by-nc-nd/2.5/

GENERATION OF FLEXURAL WAVES IN INFINITE PLATES BY LASER-INITIATED AIR SHOCK WAVES

VB Georgiev   Dept. of Aeronautical and Automotive Engineering, Loughborough University.
VV Krylov   Dept. of Aeronautical and Automotive Engineering, Loughborough University.
Q Qin   Acoustics Research Centre, Dept. of Engineering, University of Hull.
K Attenborough   Dept. of Engineering, University of Hull.

1   INTRODUCTION

Controlled explosions that take place above ground surface during military testing generate not only shock waves in air but also strong ground vibrations. It is convenient and much less expensive to study the associated sound and vibration phenomena using reduced-scale laboratory simulations, with a laser as a source of air shock waves interacting with large elastic plates modelling the ground[1,2]. Earlier, a semi-analytical model describing interaction of air shock waves with an elastic half space has been suggested by one of the present authors to describe generation of Rayleigh surface waves by electric spark discharge near the surface[3].

The aim of the present paper is to further develop the above-mentioned semi-analytical model[3] and to apply it to the interaction of laser-initiated air shock waves with an infinite elastic plate. The impact of the incident shock wave is to be approximated by an equivalent cylindrically diverging surface force resulting from the surface pressure of the incident and reflected shock waves. The well-known analytical expressions for air particle velocity and pressure in the front of a shock wave are used to describe this surface force as a function of time and distance from the epicentre. The problem is then solved using the Green's function method applied to an infinite plate. The resulting frequency spectra and time shapes of the generated flexural wave pulses are calculated for different values of the height of the laser-generated spark above the plate surface. The obtained theoretical results for time histories and frequency spectra of generated flexural waves are compared with the results of the reduced-scale model experiments on shock wave interaction with a large plastic plate.

2   THEORETICAL BACKGROUND

2.1 Specification of the Equivalent Surface Force

According to Ref. 3, the pressure in the spherically diverging air shock wave can be approximated by the following simple analytical expression:

$$P^{sh}(r,t) = P^{sh}(r)H\left(t - \int_0^r \frac{dr'}{v(r')}\right)\exp\left[-\left(t - \int_0^r \frac{dr'}{v(r')}\right)\left(\varepsilon\int_0^r \frac{dr'}{v(r')}\right)^{-1}\right],$$ (1)

Here $H(t)$ is a Heaviside step function, $v^{sh}(r)$ and $P^{sh}(r)$ are particle velocity and pressure in the front of a shock wave[4] and $\varepsilon = 0.05$ is a constant controlling the duration of the pressure pulse:

$$v^{sh}(r) = \frac{2}{5}\zeta_0^{5/2}\left(\frac{E}{\rho_0}\right)^{1/2} r^{-3/2},$$ (2)

$$P^{sh}(r) = \left(\frac{2}{5}\right)^2 \frac{2\zeta_0^5}{\gamma+1}Er^{-3},$$ (3)

E is the energy instantly released in the origin of the shock wave, ρ_0 is the mass density of the air, $\gamma \approx 1.41$ is the Poisson adiabat, and $\zeta_0 \approx 0.93$ is the dimensionless parameter characterizing the self-similar motion of the wave front[4].

As a result of interaction of the shock wave with an infinite plate, a considerable part of the incident wave energy is reflected back into the air, whereas the reminder is transformed into the energy of flexural plate vibrations. To evaluate the air pressure acting on the plate surface, the latter can be approximated as absolutely rigid. In this case, the surface pressure can be considered as the sum of the incident and reflected pressures. Using the usual linear acoustic reflection coefficient from a rigid surface (equal to 1), the resulting surface pressure can be expressed simply as twice the pressure in the incident wave[3]. Thus, the equivalent normal surface force per unit area F_n^{sh} created by the shock wave can be expressed using Eqns (1) - (3) as

$$F_n^{sh}(t,\rho) = 2P^{sh}(r)H[t - t_0^{sh}]\exp\{-[t - t_0^{sh}]/\varepsilon t_0^{sh}\},\tag{4}$$

where

$$t_0^{sh} = \left(\frac{r}{\zeta_0}\right)^{5/2}\left(\frac{\rho_0}{E}\right)^{1/2}$$

In Eqn (4), the distance r from the origin of laser-induced acoustic shock to a point of observation on the surface is equal to $\sqrt{\rho^2 + h^2}$ (see Figure 1).
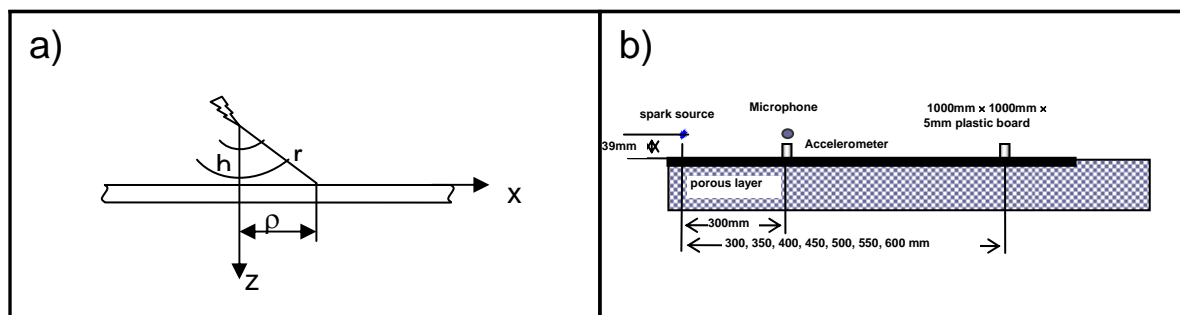

Figure 1: Interaction of laser-initiated air shock waves with a plate: (a) – geometry of the problem, (b) – experimental scheme.

For further analysis, the frequency spectrum of the normal force $F_n^{sh}(t,\rho)$ is required:

$$F_n^{sh}(\omega,\rho) = \frac{1}{2\pi}\int_{-\infty}^{+\infty} F_n^{sh}(t,\rho)\exp(i\omega t)dt\tag{5}$$

Substituting Eqn (4) into Eqn (5), this frequency spectrum can be expressed as follows:

$$F_n^{sh}(\omega,\rho) = \frac{P^{sh}(r)}{\pi}\frac{\varepsilon t_0^{sh}}{1 - i\omega\varepsilon t_0^{sh}}\exp(i\omega t_0^{sh})\tag{6}$$

2.2 Modified Equivalent Surface Force

In the previous section, the equivalent surface force (Eqn (4)) has been specified using Eqns (1)-(3). The pressure due to the air shock wave in this description is an exponential function with its maximum value depending on the distance to the center of the laser-induced spark. The time history of the air pressure pulse calculated according to Eqns (1)-(3) can be seen in Figure 2 (a). Note however that a more detailed theoretical description and measurements of pressure pulses induced by shock waves show that, when the shock front approaches a given point, the pressure initially undergoes a discontinuous jump above the atmospheric pressure. Then it decreases below the atmospheric pressure (positive and negative phases), and finally returns to its initial value[4].

In the light of the above, the initial expression (1) can be modified to model shock wave pulses more realistically. For this purpose, an additional exponential term that helps to describe the negative pressure phase can be added to Eqn (1). The air pressure can then be expressed as follows (see also Fig. 2 (b)):

$$P^{sh}(r,t) = P^{sh}(r)\left\{ \begin{array}{l} H(t-t_0^{sh})\left[1.2\exp\left(-(t-t_0^{sh})\frac{1}{\varepsilon t_0^{sh}}\right)-0.2\right]- \\ -H(t-t_0^{sh}1.25)\left[1.2\exp\left(-(t-t_0^{sh})\frac{0.36}{\varepsilon t_0^{sh}}\right)-0.2\right] \end{array} \right\}. \qquad (7)$$
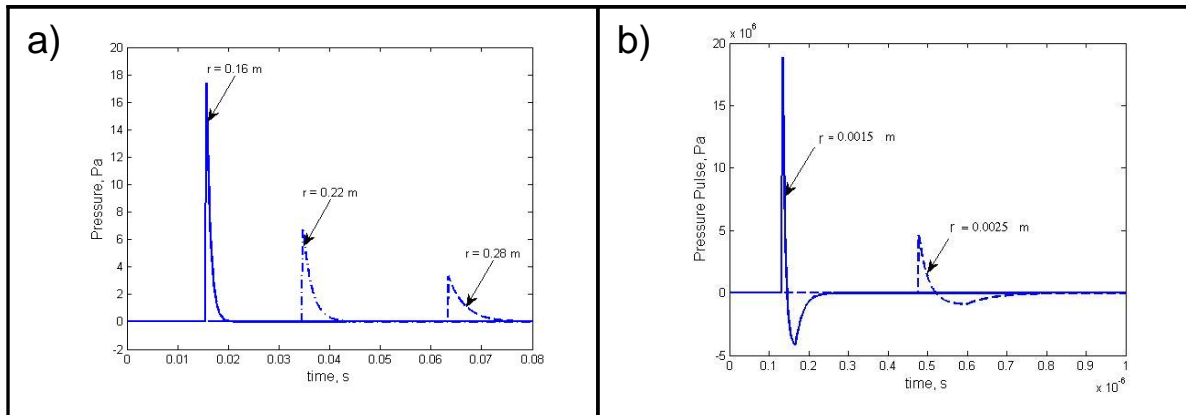

Figure 2: Air pressure pulses calculated according to Eqn (1) - (a) and to Eqn (7) – (b).

Using the above-mentioned modified expression for air pressure (Eqn (7)) and the acoustic approximation for the reflection coefficient, the equivalent surface force can be expressed as:

$$F_n^{sh}(r,t) = 2P^{sh}(r,t),$$

Using Fourier transform, the frequency spectrum of the above function can be expressed as follows:

$$F_n^{sh}(\omega,\rho) = \frac{P^{sh}(r)}{\pi}\left\{ \begin{array}{l} \frac{1.2\varepsilon t_0^{sh}}{1-i\omega\varepsilon t_0^{sh}}\exp(i\omega t_0^{sh})-\frac{0.2}{i\omega}\left[\exp\left(i\omega t_0^{sh}1.25\right)-\exp(i\omega t_0^{sh})\right]- \\ -\frac{3.36\varepsilon t_0^{sh}}{1-i\omega\varepsilon t_0^{sh}2.8}\exp\left(-\frac{0.09}{\varepsilon}+i\omega t_0^{sh}1.25\right) \end{array} \right\}. \qquad (8)$$

Note that the above expressions for the equivalent surface force (Eqns (6) and (8)) have been derived using Eqns (2) and (3) for velocity and pressure of a strong air shock wave[4]. However, for distances r that are large enough, say $r > r_0$, where r_0 is the distance at which the particle velocity at a shock front becomes equal to the speed of sound, the above-mentioned expressions for surface forces are no longer valid. Figure 3 (a) shows how particle velocity at the shock front changes with the distance from the origin.

In this case the air particle velocity and pressure beyond the distance $r_0 = 0.0084$ m (defined from Eqn (2) for $v_0 = 340$ m/s and $E = 0.8$ J is the laser energy per pulse), have to be calculated using the characteristics of a normal acoustic wave propagating with the speed of sound v_0. The wave pressure in this case is inversely proportional to the distance: $P(r) = A/r$, where the constant A should be determined by equalising the air pressure in the shock wave to the acoustic wave pressure at $r = r_0$. For an acoustic wave, Eqns (2) and (3) should be replaced by the following expressions:

$$v^{ac} = v_0 = 340 \text{ m/s}$$

$$P^{ac}(r) = \left(\frac{2}{5}\right)^2 \frac{2\zeta_0^5}{\gamma+1} \frac{E}{r_0^2 r} \tag{9}$$
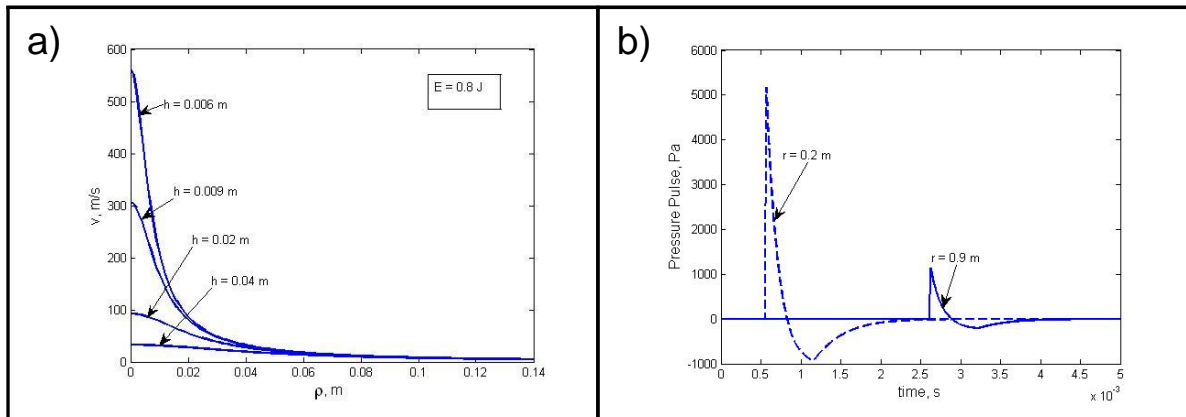

Figure 3: Shock front velocity as a function of height h of the laser spark and distance ρ from the epicenter – (a); pressure pulse in an acoustic wave according to Eqn (10) – (b).

Using the above equations, one can obtain the following expression for $r > r_0$:

$$P^{ac}(r,t) = P^{ac}(r) \left\{ \begin{array}{l} H(t - t_0^{ac})\left[1.2\exp\left(-(t - t_0^{ac})\frac{v_0}{\varepsilon}\right) - 0.2\right] - \\ - H(t - t_0^{ac} - 0.0006)\left[1.2\exp\left(-(t - t_0^{ac})\frac{150}{\varepsilon}\right) - 0.2\right] \end{array} \right\}, \tag{10}$$

where $t_0^{ac} = \dfrac{r - r_0}{v_0}$. Figure 3 (b) shows the pressure pulse according to Eqn (10).

Using again the linear acoustics approximation for the reflection coefficient, the equivalent normal surface force can be written down as the doubled incident pressure, and the frequency spectrum of the equivalent surface force can be expressed as:

$$F_n^{ac}(\omega,\rho) = \frac{P^{ac}(r)}{\pi} \left\{ \begin{array}{l} \dfrac{1.2\varepsilon}{v_0 - i\omega\varepsilon} \exp(i\omega t_0^{ac}) - \dfrac{0.2}{i\omega}\left[\exp\left(i\omega(t_0^{ac}+0.0006)\right) - \exp(i\omega t_0^{ac})\right] - \\[3mm] - \dfrac{1.2\varepsilon}{150 - i\omega\varepsilon} \exp\left(-\dfrac{0.09}{\varepsilon} + i\omega(t_0^{ac}+0.0006)\right) \end{array} \right\} \tag{11}$$

2.3   Flexural Wave Generation in an Infinite Plate

Since the problem under consideration is axisymmetric, the flexural response of the infinite plate to the spectral component of the applied normal force $F_n(x,y,\omega)$ due to the air shock wave can be described by the equation in cylindrical coordinates, with the origin at the epicentre[5]:

$$D\left(\frac{d^2}{d\rho^2} + \frac{1}{\rho}\frac{d}{d\rho}\right)^2 w - \rho_s h\omega^2 w = F_n(\omega,\rho), \tag{12}$$

where

$$F_n(\omega,\rho) = \left\{ \begin{array}{l} F_n^{sh}, 0 < r < r_0 \\ F_n^{ac}, r > r_0 \end{array} \right\}. \tag{13}$$

Here $D = \tilde{E}d^3/12(1-\nu^2)$ is bending stiffness of the plate, $\tilde{E}$ is the Young's modulus, d is the plate thickness, and ν is the Poisson's ratio. Equations (12) and (13) can be solved using the Green's function method, which yields the following expression for bending displacement in the wavenumber-frequency domain[5]:

$$\tilde{w}(\omega,k) = \frac{F_n(\omega,k)}{D(k^4 - k_f^4)}. \tag{14}$$

Here $k_f = (\rho_s h\omega^2/D)^{1/4}$ is the plate flexural wavenumber, and $F_n(\omega,k)$ is the Hankel transform of Eqn (13) which is to be calculated numerically:

$$F_n(\omega,k) = \int_0^{\rho_0} F_n^{sh}(\omega,\rho)\rho J_0(k\rho)d\rho + \int_{\rho_0}^{\infty} F_n^{ac}(\omega,\rho)\rho J_0(k\rho)d\rho \tag{15}$$

The inverse Hankel transform describes the plate response to the acoustic shock in the space-frequency domain:

$$w(\omega,\rho) = \frac{1}{D}\int_0^{\infty} \frac{F_n(\omega,k)k J_0(k\rho)dk}{k^4 - k_f^4}. $$

Expressing the Bessel function in terms of Hankel functions and using the properties of Hankel functions, the bending displacement can be rewritten as:

$$w(\omega,\rho) = \frac{1}{2D} \int_{-\infty}^{\infty} \frac{F_n(\omega,k)kH_0^{(1)}(k\rho)dk}{k^4 - k_f^4} \qquad (16)$$

The integral in Eqn (16) can be evaluated using the method of residues:

$$w(\omega,\rho) = 2\pi i \left(\frac{1}{2D} \frac{F_n(\omega,k_f)k_f H_0^{(1)}(k_f\rho)}{4k_f^3} \right), \qquad (17)$$

where the term in brackets represents the residue at $k = k_f$. Using the well-known asymptotic formula for the Hankel function at $k_f\rho >> 1$, the expression for plate vertical displacement can be written as follows:

$$w(\omega,\rho) = \frac{iF_n(\omega,k_f)}{4\omega^{5/4}\rho_s^{5/8}d^{5/8}D^{3/8}} \sqrt{\frac{2\pi}{\rho}} \exp(ik_f\rho - i\pi/4). \qquad (18)$$

This expression, combined with the harmonic time factor $e^{-i\omega t}$, represents a cylindrical flexural wave propagating from the epicenter of the acoustic shock. Obviously, the vertical components of plate particle velocity and acceleration can be obtained from Eqn (18) as:

$$\dot{w}(\omega,\rho) = -i\omega w(\omega,\rho) \quad \text{and} \quad \ddot{w}(\omega,\rho) = -\omega^2 w(\omega,\rho)$$

The time history of the displacement can be calculated from Eqn (18) using the inverse Fourier transform:

$$w(t,\rho) = \int_{-\infty}^{\infty} w(\omega,\rho)e^{-i\omega t}d\omega. \qquad (19)$$

3   EXPERIMENTAL SIMULATIONS

The rig used for the model experiments is shown in Figure 1 (b). Sparks were generated by a Q-switch Surelite III-10 Nd: YAG laser with a 1064 nm wavelength and the energy of 0.8 J per pulse. For the measurements of flexural vibrations, a DJB A/20 accelerometer with the mass 18 g, sensitivity 35 pC/g and resonant frequency 28 kHz was used. The plate was made of laminated plastic material. Its horizontal dimensions and thickness were 1x1 m^2 and 0.005 m respectively. Measurements were carried out for two heights of the laser generated spark over the plate surface: 0.039 m and 0.003 m. The accelerometer was placed at two distances from the epicentre: 0.3 m and 0.6 m. Further details about the laboratory equipment and test rig can be found in Refs 1 and 2.

4   COMPARISON OF THE THEORETICAL AND EXPERIMENTAL RESULTS

In this section some of the results of theoretical modelling and experimental simulations are presented and compared (see Figures. 4 and 5). The material characteristics used in the analytical calculations are as follows: mass density $\rho_s = 900$ kg/m^3, Young's modulus $\widetilde{E} = 50.10^8$ N/m^2, Poisson's ratio $\nu = 0.3$.
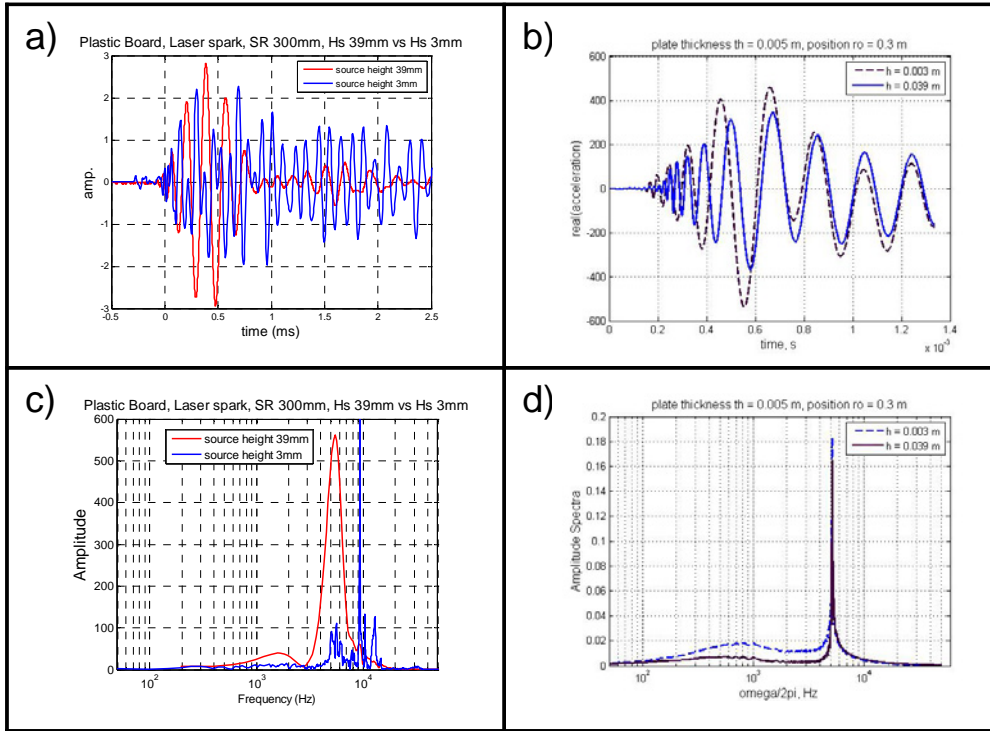
Figure 4: Time history ((a), (b)) and amplitude spectra ((c), (d)) of the plate acceleration at distance 0.3 m away from the epicenter: measured ((a), (c)) and calculated ((b),(d)).
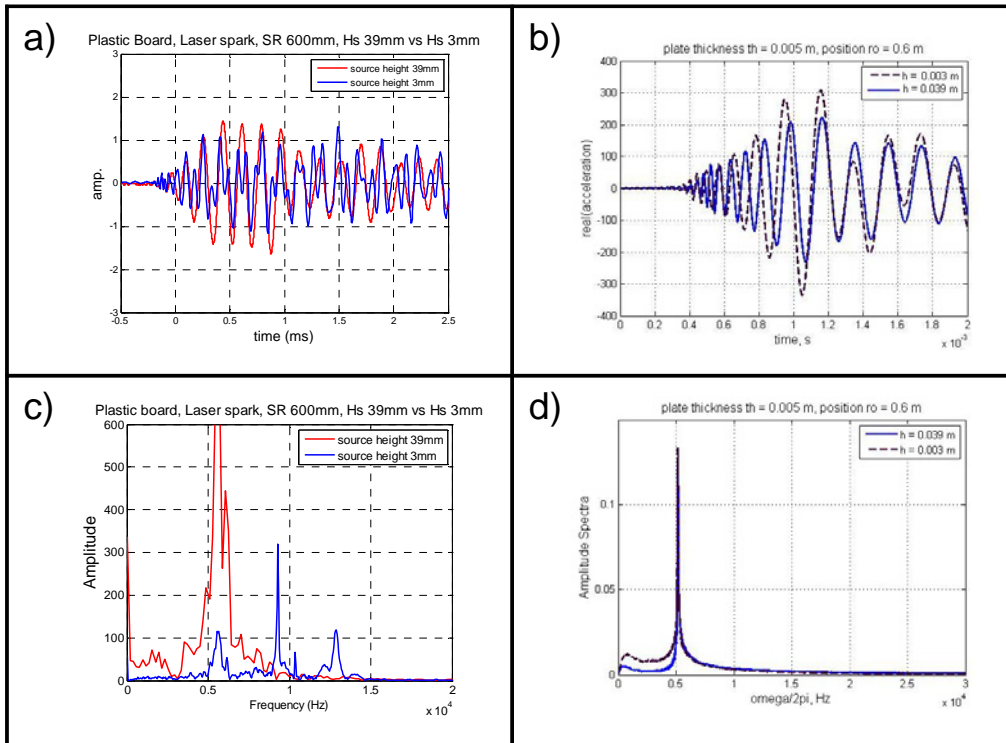

Figure 5: Time history ((a), (b)) and amplitude spectra ((c), (d)) of the plate acceleration at distance 0.6 m away from the epicenter: measured ((a), (c)) and calculated ((b),(d)).

The results shown in Figures 4 and 5 represent the time histories and amplitude spectra of the plate acceleration at distance 0.3 m and 0.6 m away from the epicenter. The height of the laser-generated spark above the plate is 0.039 m and 0.003 m. Both series of graphs, experimental and theoretical, show oscillations at frequency about 5 kHz. Apparently, this behaviour is due to a coincidence phenomenon, when sound waves incident on a plate at a particular angle have a trace wavelength matching exactly to that of the plate bending wave.

The experimental frequency spectra at h = 0.039 m are broader than the theoretical ones. At h = 0.003 m the coincidence frequency is shifted slightly towards higher frequencies and some new peaks appear, whereas the theoretical ones do not change significantly. It was assumed that these discrepancies could be attributed to non-linear effects associated with reflection of shock waves. The non-linear reflection of shock waves has been taken into account in the later stage of this investigation using the well-known analytical formula for shock wave reflection from a rigid surface[6]. It has been shown, however, that taking into account the non-linear reflection simply increases the amplitude and slightly changes the shape of the pressure pulse, mainly in the zone of strong shocks. Beyond the critical distance r_0, the part of the pressure associated with non-linear reflection is small in comparison with that due to the linear one. As a result, the calculated time histories and amplitude spectra of the plate flexural waves do not differ significantly from those calculated using linear reflection. The only difference is in slightly increased amplitudes of the frequency spectra and time histories when non-linear reflection is taken into account.

5   CONCLUSIONS

In the present paper, a semi-analytical model of flexural wave generation in an infinite plate due to laser-initiated air shock waves has been developed. Analysis of the obtained results shows that the coincidence condition plays an important role in the observed phenomena, being responsible for harmonic oscillations around the coincidence frequency. The comparison of calculated theoretical results and experimentally observed data has shown reasonably good agreement. This proves that the developed semi-analytical model is reliable enough for prediction of flexural wave generation in an infinite plate due to laser-initiated air shock waves. Some observed discrepancies between experimental and theoretical results may be caused by different wave generation and propagation mechanisms that require further attention.

6   ACKNOWLEDGEMENT

7   REFERENCES

1.   K. Attenborough and Q. Qin, Model experiments on shock wave interaction with the ground, Proceedings of the 19th ICA, Madrid, Spain, 2-7 September 2007 (on CD).
2.   Q. Qin and K. Attenborough, Characteristics and application of laser-generated acoustic shock waves in air, Applied Acoustics, 65, 325-340 (2004).
3.   V.V. Krylov, On the theory of surface acoustic wave generation by electric spark discharge, J. Phys. D: Appl. Phys., 25, 155-161 (1992).
4.   Y.B. Zel'dovich and Y.P. Raizer, Physics of shock waves and high temperature hydrodynamic phenomena, Vols 1, 2, New York: Academic Press (1966, 1967).
5.   M.C. Junger and D. Feit, Sound, structures and their interaction, Cambridge: MIT Press (1972).
6.   J.K. Wright, Shock tubes, New York: Wiley&Sons (1961).